Tailoring the ultrafast dynamics of the magnetic mode in magnetic photonic crystals

M. Geiselmann,[1,2] T. Utikal,[1,2] M. Lippitz,[1,2] and H. Giessen[1]
[1]*4th Physics Institute, University of Stuttgart, Pfaffenwaldring 57, 70550 Stuttgart, Germany*
[2]*Max Planck Institute for Solid State Research, Heisenbergstraße 1, 70569 Stuttgart, Germany*
(Received 24 March 2010; revised manuscript received 3 May 2010; published 1 June 2010)

We investigate the ultrafast time dynamics of magnetic waveguide-particle-plasmon polaritons in a magnetic photonic crystal. This magnetic mode consists of the antisymmetric localized charge oscillation in metallic cut-wire pairs. At the appropriate periodicity, strong coupling and polaritonic hybridization take place between the antisymmetric plasmon resonance and the excited photonic mode of the underlying slab waveguide. By varying the lattice period and the wire cross section of the structure, tailoring of the temporal dynamics of the magnetic polariton is possible. Simulations are in good agreement with third-order nonlinear autocorrelation function measurements and confirm extremely long dephasing times of the polaritonic system. Future applications could include all-optical control of optical magnetism.

DOI: 10.1103/PhysRevB.81.235101 PACS number(s): 42.70.Qs, 78.47.−p, 73.20.Mf

I. INTRODUCTION

In recent years the ultrafast time dynamics of plasmonic resonances in metal nanostructures has become a center of interest in nanoscience.[1–3] For nano-optics and nanodevices such as optical switches these temporal dynamics are of crucial importance.[4,5] The temporal dynamics were previously studied on surface plasmon polaritons,[6,7] which are propagating surface waves on continuous metallic films. However, surface plasmon polaritons need to be distinguished from particle plasmon polaritons, which are localized electron oscillations in nanosized metal structures. These particle plasmon polaritons can easily be excited by an external light field.[8] In particular the dephasing of this oscillation is of interest, because the dephasing time T_2 is proportional to the local field enhancement.[9,10] This is of crucial importance for surface-enhanced Raman spectroscopy.[11] Unfortunately, due to efficient coupling of the particle plasmon to the vacuum light modes, the radiative damping is very high and therefore the oscillation decays very fast.[12,13] This is why the dephasing time T_2 defined by $1/T_2=1/(2T_1)+1/T_2^*$ is dominated by the radiative dephasing $2T_1$ and the pure dephasing T_2^*, which is of the order of a few picoseconds and thus can be neglected. First experiments on gold nanoparticles determined the dephasing time to be in the range of a few femtoseconds.[14–16] In 2004 Zentgraf *et al.*[17] circumvented this problem by coupling the plasmon resonance of gold nanostructures to a photonic slab waveguide mode. Consequently the density of states of the new hybrid system, termed a waveguide-plasmon polariton[18] (WPP), was modified and dephasing times up to 50 fs were found.[17]

So far, only *electric* dipole resonances were investigated. However, plasmonics recently has moved to metamaterials and structures with periodically arranged magnetic building blocks, termed "magnetic photonic crystals,"[19] providing an electric quadrupole and thus a *magnetic dipole moment* in the *optical frequency range*.[20] In these structures, such as split ring resonators and cut-wire pairs, electric ring currents can be excited by an external electromagnetic light field. These ring currents cause magnetic dipole moments in the perpendicular direction, which constitute magnetic resonances at optical frequencies, sometimes also termed "optical magnetism."

Here, we experimentally and theoretically demonstrate the influence of polaritonic hybridization[21] on the temporal dynamics of magnetic resonances in subwavelength metal nanostructures. The dynamics are tailored by coupling the magnetic resonances to a photonic waveguide mode. We show that changing the coupling strength between the magnetic resonances and the waveguide mode leads to significant changes in the temporal dynamics with dephasing times up to 80 fs. This could pave the way to all-optically control optical magnetism, which could be switched on and off on a 10 fs time scale. Doing so would imply to utilize an ultrafast three-pulse experiment to excite the antisymmetric mode in a cut-wire pair. Within its dephasing time, a second, phase-stabilized pulse would coherently create or destroy that plasmonic polarization. With a third pulse, the amount of optical magnetism, i.e., the remaining polarization, could be interrogated. This effect has recently been demonstrated for electric resonances in plasmons.[22] Furthermore, due to the long dephasing the linewidth of the polaritonic resonances is reduced, which enables tailoring the magnetic resonance for many applications in plasmonics, especially for sensing.

II. SAMPLES AND NUMERICAL DISCUSSION

In this work the magnetic resonance is provided by the antisymmetric mode of a gold double wire structure. For studying the coupling to photonic modes and the resulting polaritonic hybridization, we periodically arrange the wires on a hafnium dioxide (HfO_2) waveguide slab and vary their periodicity P_x and wire width d (Fig. 1). This will also modify the temporal dynamics of the system. We fabricate several arrays of these magnetic building blocks by electron beam lithography on a quartz substrate with the 160 nm thick HfO_2 waveguide slab on top. Linden *et al.* introduced this structure as a *magnetic photonic crystal* in the near infrared.[19] A slice of the structure was cut out using focused ion beam milling and investigated with a scanning transmission electron microscope. As shown in Fig. 2(a) the 100 nm thick double wire building block is periodically arranged on

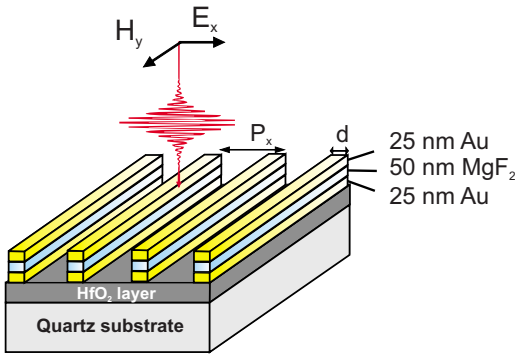

FIG. 1. (Color online) Scheme of the magnetic photonic crystal with a double wire gold structure on top of a HfO_2 slab waveguide. The polarization of the incident electric field is perpendicular to the wires.

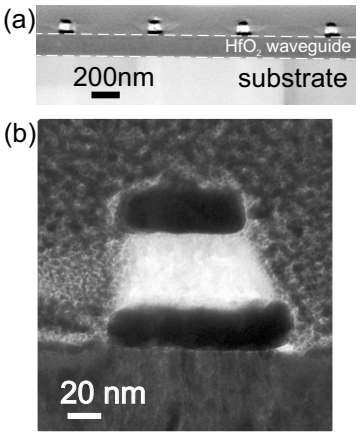

FIG. 2. (a) Scanning transmission electron microscope (TEM) picture of a sample grating line on a waveguide slab cut with focused ion beam. (b) TEM picture of one single "magnetic atom" consisting of two 25 nm thick gold wires separated by a 50 nm thick magnesium fluoride spacer.

the waveguide. Periods are varied from 480 nm to 580 nm. In Fig. 2(b) a single magnetic building block is shown. The 25 nm thick gold wires are separated by a 50 nm magnesium fluoride (MgF_2) spacer layer. The wire width of the upper wire differs from the bottom wire due to the lift-off fabrication process. This facilitates optical excitation of the antisymmetric magnetic mode. We investigate two sets of samples. In a first set of samples, the bottom wire width d is fixed and the grating period P_x is varied. In a second set, the period P_x is fixed and the wire width d is varied. To get insight into the optical response of the structure, we numerically simulate the linear spectrum with a scattering matrix approach.[23,24] In Fig. 3(a) the simulated extinction spectrum is plotted versus the grating period P_x for a fixed wire width $d=100$ nm.

First we discuss the regime for small grating periods (i.e., smaller than 300 nm). For the incident light with its polarization perpendicular to the wire pairs (see Fig. 1) two modes are excited in the optical regime. One is a symmetric mode at short wavelengths (white line at $\lambda=575$ nm), where the electric field in the two gold wires is oriented in the same direction. This mode has electric dipole character. The other mode is an antisymmetric mode (white line at $\lambda=704$ nm), where the electric field in the gold wires points in opposite directions. It can be regarded as the magnetic mode. Here the magnetic field is concentrated in the MgF_2 spacer and oriented along the wires.[19] The finite size of the "magnetic atom" is one reason why the antisymmetric mode is optically excitable. In order to excite the antisymmetric mode in a cut-wire pair, symmetry breaking has to occur. The symmetry in z direction is broken, as the upper gold wire has an air interface and the bottom gold wire has a dielectric interface. This leads to a change in the refractive index and thus to a symmetry breaking. Additionally the structure has a trapezoidal shape (Fig. 2) and the phase lag of the incident wave between the upper and lower wire enables coupling due to retardation effects.[25]

Second, we consider the regime for periods between 300 and 450 nm. In this case, the photonic waveguide mode (white tilted line) can be excited in the same wavelength range as the plasmonic modes and interacts with them. For

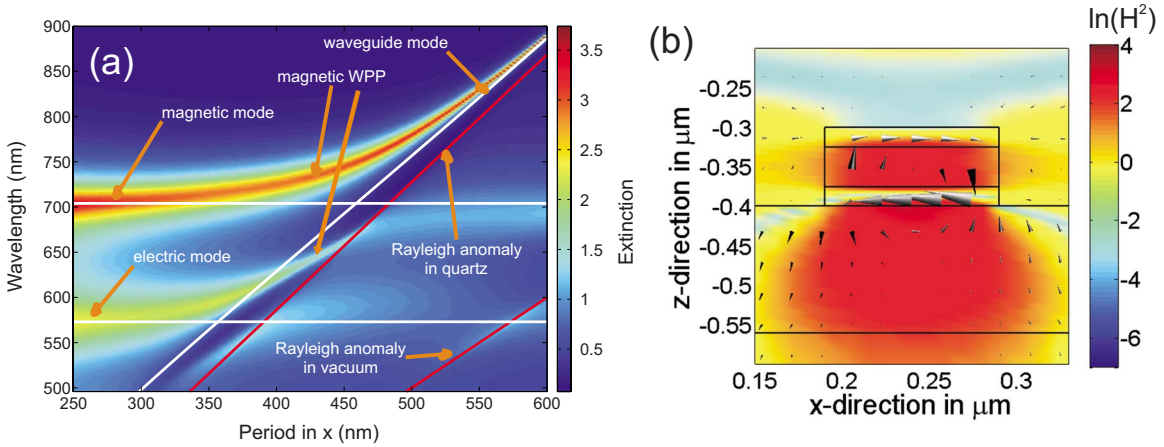

FIG. 3. (Color online) (a) Extinction (Ext$=-\ln T$) of the magnetic photonic crystal plotted versus the wavelength and the grating period. (b) Field distribution of a double wire structure ($\lambda=763$ nm and $P_x=480$ nm). The arrows show the electric field distribution. The magnetic field is plotted as a color map, defined as $\ln(\mathbf{H}^2)$ and $\mathbf{H}_{\text{incident}}=1$. The concentration of the magnetic field in the spacer and the waveguide represents the magnetic polariton character.

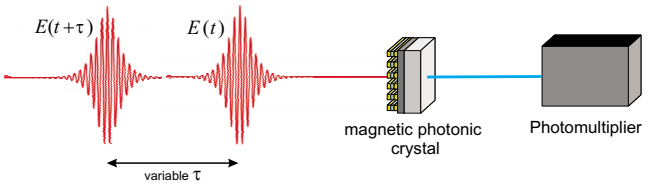

FIG. 4. (Color online) Two pulses delayed by a time τ hit the sample and generate the third harmonic. The intensity of the THG is measured with a photomultiplier. The intensity plotted over the time delay τ gives the autocorrelation function of the sample.

periods around 350 nm the photonic mode strongly couples to the electric mode, which leads to an anticrossing. In the strong coupling regime the plasmonic electric mode is hybridized to a waveguide-plasmon polariton.[18] For larger periods the longer wavelength polariton branch changes its character from an electric polariton branch to a magnetic polariton branch as the photonic waveguide mode now couples strongly with the magnetic mode, which also leads to an anticrossing.

Third, we study periods P_x from 480 to 580 nm. In this case, the photonic waveguide mode only couples to the magnetic plasmon resonance. As this waveguide mode possesses long dephasing times, the coupling between the photonic mode and the plasmonic modes is used to tailor the time dynamics. For periods larger than 480 nm only the magnetic mode is hybridized comparably to the electric mode for smaller periods. Hence, the new system is termed "magnetic waveguide-(particle-)plasmon-polariton (MWPP)." The magnetic field at 763 nm wavelength and P_x=480 nm is plotted as a color map in Fig. 3(b). Owing to the electric ring currents (black arrows), the magnetic field is mainly concentrated in the MgF_2 spacer and the HfO_2 slab waveguide, which confirms the magnetic polaritonic character of the mode.

III. EXPERIMENTAL AND THEORETICAL RESULTS

A. Tailoring dynamics via grating period

We experimentally investigate three cases of coupling, where the wire width is fixed and the grating period P_x is varied. In Figs. 5(a)–5(c) extinction spectra are shown for three different grating periods. A change in the grating period from 480 to 580 nm results in a red shift of the photonic waveguide mode and also leads to a red shift of the MWPP branches. Besides the spectral shift, there is also a change in the linewidth of the two polariton branches. Hence a change in the dephasing time T_2 is also expected.

For studying the temporal dynamics of the MWPP we use a third-order nonlinear interferometric autocorrelation technique. A Ti:sapphire laser generates 8 fs pulses at a center wavelength of 800 nm with a repetition rate of 150 MHz. The laser spectrum is plotted in gray in Figs. 5(a)–5(d). In a stabilized Michelson interferometer[26,27] the pulses are split up and time-delayed with respect to each other and subsequently focused on the sample. We detect the third harmonic light as a function of the time delay τ.[28] A schematic of the setup is shown in Fig. 4.

In Figs. 5(e)–5(g) the measured autocorrelation functions (ACFs) of the three arrays are displayed. The broadening of the ACF stretches from below 20 to over 60 fs, strongly depending on the periodicity of the samples. These measurements excellently display the dynamics in the time domain.

The local electric field of the particle plasmon can be modeled by a damped harmonic oscillator as described in Lamprecht *et al.*[14] In contrast to an undisturbed particle plasmon, the MWPP spectrally splits into two polariton branches, with each branch j having a specific dephasing time T_2^j. The resonance frequencies ω_j were taken from the extinction spectrum of the MWPP. Then the plasmon field $E_p(t)$ is proportional to

$$E_p(t) \propto \int_{-\infty}^{t} \sum_j \frac{A_j}{\omega_j} K(t') e^{-\gamma j(t-t')} \sin[\omega_j(t-t')] dt', \quad (1)$$

where $K(t')$ denotes the driving force, A_j is the oscillator strength, and $\gamma_j = 1/T_2^{(j)}$ is the damping of the resonance ω_j. $K(t')$ is given by the coherent sum of the two laser pulse fields $E_{\text{light}}(t)+E_{\text{light}}(t+\tau)$ from the interferometer. The theoretical third-order ACF can be obtained by taking the sixth power of the absolute value of $E_p(t)$ for each τ and integrating over time. The temporal dynamics of the MWPP were determined by fitting the experimentally obtained ACF with Eq. (1) using A_j and γ_j as fit parameters. We use the measured laser spectrum of the bare laser pulses as the input driving field $E(t)$. The related simulated ACF are plotted in Figs. 5(i)–5(k). We find excellent agreement between the simulations and the experimental data.

For a period of 480 nm we obtain a dephasing time of $T_2^{(1)}$=24 fs from the parameter fits for the longer wavelength polariton branch. For a period of 530 nm the dephasing time $T_2^{(1)}$ is increased to 60 fs for the same branch. At a period of 580 nm the dephasing time is further increased to $T_2^{(1)}$=80 fs. These values can be determined with an accuracy of about 10%.

By varying the grating period P_x, the coupling between the plasmon mode and the waveguide mode is modified, which leads to changes in the dynamics and the dephasing of the polaritonic system. The longer wavelength branch of the MWPP is more plasmonlike for shorter periods and becomes more waveguidelike for larger periods. For larger periods this means that the field is stored in the waveguide with a higher quality factor. This leads to a sharper linewidth of the longer wavelength polariton branch and simultaneously to a longer dephasing time $T_2^{(1)}$. At P_x=530 nm, the longer wavelength branch is more waveguidelike and the dephasing time increases compared to the polariton branch of the structure with a grating period of 480 nm. Simultaneously its oscillator strength, plotted as inset in Figs. 5(i)–5(k), becomes smaller since this polariton branch is less plasmonlike. Therefore, the dephasing time increases up to $T_2^{(1)}$=80 fs for a period of 580 nm but the oscillator strength $A^{(1)}$ diminishes from 0.8 to 0.04.

There is also a second factor that contributes to the dynamics: only if the laser is resonant to the MWPP, a broad autocorrelation is observed [Fig. 5(j)]. For less resonant ex-

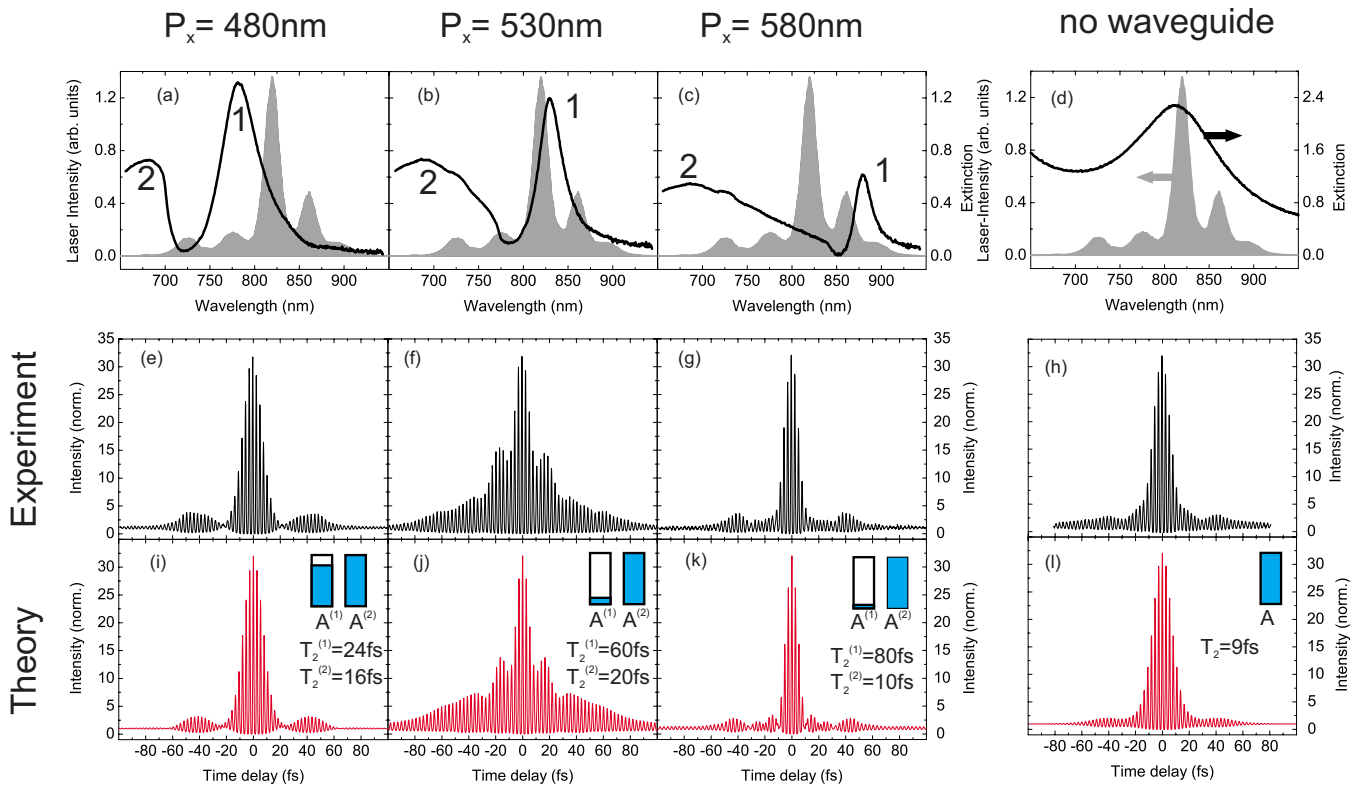

FIG. 5. (Color online) (a)–(c) Extinction spectra, (e)–(g) measured, and (i)–(k) calculated nonlinear ACFs of three different arrays on an HfO_2 waveguide. Fixing the wire width at 100 nm, the grating period varies from 480 to 530 and 580 nm. The obtained values for the dephasing times $T_2^{(i)}$ of the polariton branches are shown as inset in (i)–(l). The bars indicate the oscillator strength of each polariton branch. Data from a double wire structure without a waveguide, a wire width of 160 nm and a period P_x=400 nm are displayed in (d), (h), and (l). The autocorrelations are symmetric around τ=0. Also the relation of 32:1 between the signal at τ=0 and large delay times is achieved. This indicates that the sample is not damaged during the measurement with the high pulse energies as well as accurate alignment of the interferometer.

citations, we still obtain a narrow autocorrelation even if the dephasing time is high [Fig. 5(k)].

B. Control experiment with no waveguide

As a control experiment, we fabricate a double wire structure without a waveguide underneath. Hence, we exclude the coupling to the waveguide mode. Due to the change of the refractive index ($n_{HfO_2} \neq n_{quartz}$) the wire width has to be increased to shift the plasmon resonance into the laser spectrum. The extinction spectrum is shown in Fig. 5(d). The broad magnetic resonance is centered at 800 nm. The sample without waveguide has an almost instantaneous response to the laser pulses. In comparison to the coupled waveguide-plasmon polariton, the bare magnetic plasmon mode shows a very narrow ACF [Fig. 5(h)]. The associated dephasing times are up to a factor of ten shorter than in the hybridized MWPP system above.

C. Tailoring dynamics via wire width

In the second set of samples the wire width is varied while the grating period is fixed. The increased wire width shifts the plasmon resonances into the red. In a corresponding dispersion diagram [similar to Fig. 3(a)] the two plasmon resonances, plotted as white horizontal lines, shift to longer wavelengths, whereas the waveguide mode remains at its value for a constant period of P_x=530 nm. Thus the coupling between the magnetic plasmon mode and the photonic waveguide mode changes and can be tailored appropriately for hybridization. This leads to a change in the dynamics as shown in Fig. 6. In Figs. 6(a)–6(c) the extinction measurements of three different arrays are plotted in black. The polariton is shifted through the laser spectrum, which is plotted in gray. The increased linewidth of the polariton branch is a result of the different coupling strengths between waveguide mode and magnetic plasmon mode. The ACF in Figs. 6(d)–6(f) show the variation of the dynamics for the different coupling. For a wire width of 100 nm and a grating period fixed at 530 nm the measured ACF is broadened compared to the ACF of the control sample. We obtain a dephasing time $T_2^{(1)}$=72 fs from the parameter fits. By increasing the wire width, the longer wavelength polariton branch obtains a more plasmonic character, as the magnetic plasmon resonance is shifted away from the waveguide mode. Thus the dephasing time $T_2^{(1)}$ diminishes to 18 fs for a wire width of 160 nm. Additionally the oscillator strength is increased. As before the simulations are in good agreement with the measured ACF.

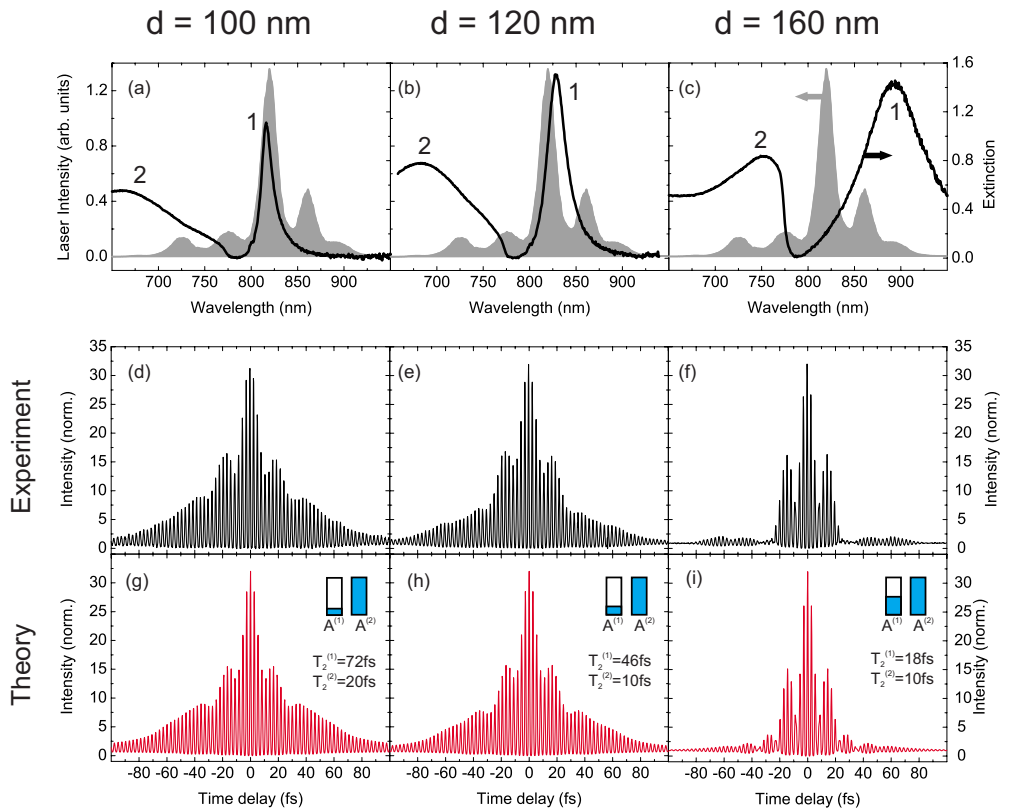

FIG. 6. (Color online) Tailoring the magnetic polariton by varying the wire width at a constant period P_x=530 nm. (a)–(c) Extinction spectra (black) and laser spectrum (gray). (d)–(f) Measured ACFs. (g)–(i) Simulated ACFs. The ACF show a beating of the autocorrelation signal. The beating period is in good agreement with the spectral distance of the two polariton branches.

IV. CONCLUSION

In conclusion, we have shown the first temporally resolved measurements of the ultrafast time dynamics of MW-PPs, even in the visible wavelength range. By changing the coupling and polaritonic hybridization of plasmonic and photonic modes the temporal dynamics are drastically modified. With a perfect agreement between simulation and experiment we found dephasing times between 24 and 80 fs.

Spectrally and temporally resolved ACF will give more information about the dynamics of the different third harmonic components in the future. These are the first steps toward all-optical control of optical magnetism as well as ultrafast plasmonic switching and novel plasmonic sensing.

ACKNOWLEDGMENTS

The authors thank B. Fenk for technical assistance. This work was financially supported by the German Bundesministerium für Bildung und Forschung (Grants No. FKZ 13N9155 and No. 13N10146), the Deutsche Forschungsgemeinschaft (Grants No. FOR 730 and No. FOR557), and the Landesstiftung Baden Württemberg.

[1] J. Becker, I. Zins, A. Jakab, Y. Khalavka, O. Schubert, and C. Soennichsen, Nano Lett. **8**, 1719 (2008).
[2] M. W. Klein, T. Tritschler, M. Wegener, and S. Linden, Phys. Rev. B **72**, 115113 (2005).
[3] F. Stietz, J. Bosbach, T. Wenzel, T. Vartanyan, A. Goldmann, and F. Trager, Phys. Rev. Lett. **84**, 5644 (2000).
[4] E. Ozbay, Science **311**, 189 (2006).
[5] K. MacDonald, Z. Samson, M. Stockman, and N. Zheludev, Nat. Photonics **3**, 55 (2009).
[6] C. Ropers, D. J. Park, G. Stibenz, G. Steinmeyer, J. Kim, D. S. Kim, and C. Lienau, Phys. Rev. Lett. **94**, 113901 (2005).
[7] J. Li, H. Iu, D. Y. Lei, J. T. K. Wan, J. B. Xu, H. P. Ho, M. Y. Waye, and H. C. Ong, Appl. Phys. Lett. **94**, 183112 (2009).
[8] U. Kreibig and M. Vollmer, *Optical Properties of Metal Clusters* (Springer-Verlag, Berlin, 1995).
[9] V. Myroshnychenko, E. Carbó-Argibay, I. Pastoriza-Santos, J. Pérez-Juste, L. Liz-Marzán, and F. G. de Abajo, Adv. Mater. (Weinheim, Ger.) **20**, 4288 (2008).
[10] F. Hao, Y. Sonnefraud, P. Dorpe, S. Maier, N. Halas, and P. Nordlander, Nano Lett. **8**, 3983 (2008).
[11] S. Lal, S. Link, and N. Halas, Nat. Photonics **1**, 641 (2007).
[12] S. Maier, *Plasmonics: Fundamentals and Applications* (Springer, New York, 2007).
[13] L. Novotny and B. Hecht, *Principles of Nano-Optics* (Cambridge

Univeristy Press, Cambridge, England, 2006).
[14] B. Lamprecht, J. R. Krenn, A. Leitner, and F. R. Aussenegg, Phys. Rev. Lett. **83**, 4421 (1999).
[15] B. Lamprecht, J. Krenn, A. Leitner, and F. Aussenegg, Appl. Phys. B: Lasers Opt. **69**, 223 (1999).
[16] C. Sönnichsen, T. Franzl, T. Wilk, G. von Plessen, J. Feldmann, O. Wilson, and P. Mulvaney, Phys. Rev. Lett. **88**, 077402 (2002).
[17] T. Zentgraf, A. Christ, J. Kuhl, and H. Giessen, Phys. Rev. Lett. **93**, 243901 (2004).
[18] A. Christ, S. G. Tikhodeev, N. A. Gippius, J. Kuhl, and H. Giessen, Phys. Rev. Lett. **91**, 183901 (2003).
[19] S. Linden, M. Decker, and M. Wegener, Phys. Rev. Lett. **97**, 083902 (2006).
[20] C. M. Soukoulis, S. Linden, and M. Wegener, Science **315**, 47 (2007).
[21] E. Prodan, C. Radloff, N. J. Halas, and P. Nordlander, Science **302**, 419 (2003).
[22] T. Utikal, M. I. Stockman, A. P. Heberle, M. Lippitz, and H. Giessen, Phys. Rev. Lett. **104**, 113903 (2010).
[23] S. G. Tikhodeev, A. L. Yablonskii, E. A. Muljarov, N. A. Gippius, and T. Ishihara, Phys. Rev. B **66**, 045102 (2002).
[24] T. Weiss, N. A. Gippius, S. Tikhodeev, G. Granet, and H. Giessen, J. Opt. A, Pure Appl. Opt. **11**, 114019 (2009).
[25] T. Meyrath, T. Zentgraf, C. Rockstuhl, and H. Giessen, Appl. Phys. B: Lasers Opt. **93**, 107 (2008).
[26] S. Pancharatnam, Proc. Indian Acad. Sci., Sect. A **44**, 247 (1956).
[27] M. U. Wehner, M. H. Ulm, and M. Wegener, Opt. Lett. **22**, 1455 (1997).
[28] T. Utikal, T. Zentgraf, J. Kuhl, and H. Giessen, Phys. Rev. B **76**, 245107 (2007).